LETTERS

A frequency comb in the extreme ultraviolet

Christoph Gohle[1], Thomas Udem[1], Maximilian Herrmann[1], Jens Rauschenberger[1], Ronald Holzwarth[1], Hans A. Schuessler[1], Ferenc Krausz[1,2] & Theodor W. Hänsch[1,2]

Since 1998, the interaction of precision spectroscopy and ultrafast laser science has led to several notable accomplishments. Femtosecond laser optical frequency 'combs' (evenly spaced spectral lines) have revolutionized the measurement of optical frequencies[1,2] and enabled optical atomic clocks[3]. The same comb techniques have been used to control the waveform of ultrafast laser pulses, which permitted the generation of single attosecond pulses[4], and have been used in a recently demonstrated 'oscilloscope' for light waves[5]. Here we demonstrate intra-cavity high harmonic generation in the extreme ultraviolet, which promises to lead to another joint frontier of precision spectroscopy and ultrafast science. We have generated coherent extreme ultraviolet radiation at a repetition frequency of more than 100 MHz, a 1,000-fold improvement over previous experiments[6]. At such a repetition rate, the mode spacing of the frequency comb, which is expected to survive the high harmonic generation process, is large enough for high resolution spectroscopy. Additionally, there may be many other applications of such a quasi-continuous compact and coherent extreme ultraviolet source, including extreme ultraviolet holography, microscopy, nanolithography and X-ray atomic clocks.

For more than three decades, laser physics and laser spectroscopy have evolved along two seemingly opposite and disconnected frontiers, pursued by different communities of researchers. In the field of high resolution spectroscopy, scientists have learned to build ultra-stable continuous wave (c.w.) laser sources and they have perfected spectroscopy of laser-cooled atomic systems to reach extremely high spectral resolution[7]. In the field of ultrafast science, researchers have demonstrated ever-shorter pulses from mode-locked laser systems and ways of amplifying such pulses to very high intensities[8]. By focusing intense amplified pulses into a gas, coherent radiation down to the X-ray region can be generated by high harmonic generation (HHG)[9]. Since this process requires very high intensities ($>10^{13}\,\mathrm{W\,cm^{-2}}$), the available laser power had to be concentrated into a small number of ultrashort pulses per second, limiting repetition rates for HHG to typically a few kHz.

To overcome this limitation, we couple the driving laser pulses from the oscillator into a high finesse optical resonator that contains the nonlinear medium. Inside this resonator, the circulating power is enhanced by a factor P (the resonator finesse divided by π) so that it can drive the nonlinear process (HHG) inside a gas target. For c.w. lasers, resonators with a finesse exceeding 100,000 can be constructed[10] and overall nonlinear conversion efficiencies approaching unity can be achieved[11]. In the case of a mode-locked ultrafast laser, however, complying with the extra requirements discussed below is more difficult: the output spectrum of a mode-locked laser contains not just a single c.w. mode but a comb of such modes, with frequencies

$$\omega_n = n\omega_\mathrm{r} + \omega_\mathrm{CE} \qquad (1)$$

Here ω_r is the pulse repetition frequency and ω_CE the carrier envelope (CE) frequency[12]. Both ω_r and ω_CE reside in the radio frequency domain, whereas the optical frequencies of the comb are given by ω_n. The two frequency regions are connected by virtue of the large integer $n = 10^5 \ldots 10^6$ that enumerates the modes. An optical resonator for such radiation has to be simultaneously resonant for each mode ω_n that originates from the laser. This can be accomplished with a resonator of appropriate length and zero group velocity dispersion, whose CE frequency is matched to the laser[13,14]. Rephrased into time domain language, coherent pulse addition in a resonator occurs if (1) the round trip time of the pulse is the same as the period of the laser, (2) the pulse envelope does not change its shape during one round trip, and (3) the carrier phase shift with respect to the envelope of the circulating pulse is the same per round trip as the pulse to pulse change from the laser. For increasing finesse, the stored pulse undergoes an increasing number of round trips and therefore dispersion compensation becomes more critical. Nevertheless, such cavities have been demonstrated to enhance nonlinear conversion for 100-fs pulses[15], and recently a resonator for sub-50-fs pulse duration has been demonstrated to provide an enhancement factor of up to 70, resulting in pulse energies of more than 200 nJ (ref. 16).

Instead of dumping the power from the resonator as has been done in earlier experiments[16], we have placed a low-density xenon gas target as the nonlinear medium for HHG inside such a resonator. In contrast to the usual HHG schemes, the power that is not converted into the extreme ultraviolet (XUV) after a single pass through the medium is 'recycled' and can contribute in subsequent passes, so that higher total conversion efficiencies than for conventional schemes can be expected. Moreover, it becomes possible to use the high power at the full repetition rate of the laser. As a result, in addition to the comb of odd laser harmonics that stem from the periodicity of the carrier wave in one pulse, a nested frequency comb with a spacing given by the repetition frequency originates from the periodic pulse train. If the HHG spectrum contains only frequency components that are the sum of the original frequencies from equation (1), as expected from energy conservation, then the XUV comb structure of the kth laser harmonic (that is, the sum of k laser photons) is given by

$$\omega'_n = n\omega_\mathrm{r} + k\omega_\mathrm{CE} \qquad (2)$$

where the integer n now runs over k times larger values than in equation (1). With such a widely spaced frequency comb, single modes that are effectively c.w. lasers may be isolated for high resolution spectroscopy. If a mode ω_n of the comb is tuned into resonance with a two-photon transition, any pair $\omega_{n-\ell} + \omega_{n+\ell}$ (with integer ℓ) is simultaneously resonant. This allows the use of the entire (broadband) power of the comb while maintaining the linewidth of a single mode[17].

Direct frequency comb spectroscopy has been applied to atomic resonances in the infrared[18–20] and in the ultraviolet range[21], and a resolution approaching the natural linewidth with a laser-cooled sample has been reached[18,20]. At the same time, the frequency comb may be phase coherently linked to a Cs atomic clock for accurate

[1]Max-Planck-Institut für Quantenoptik, Hans-Kopfermann-Strasse 1, [2]Department für Physik der Ludwig-Maximilians-Universität München, Am Coulombwall 1, D-85748 Garching, Germany.

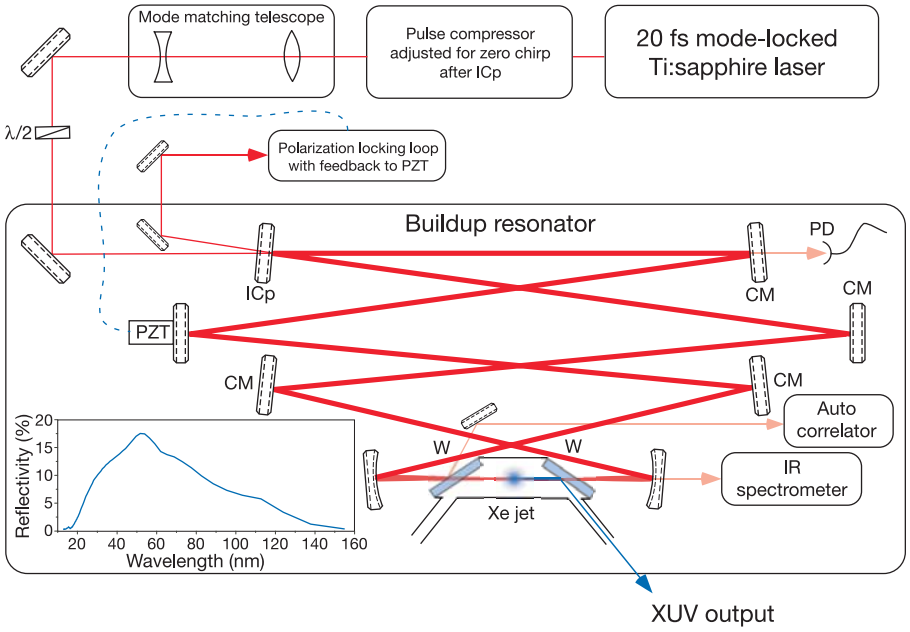

Figure 1 | The XUV laser set-up. ICp, coupling mirror with 1% transmission; CM, chirped mirrors; PD, photodiode; W, Brewster-angled sapphire window of 1 mm thickness; PZT, piezoelectric transducer. Inset shows the reflectance of sapphire for p-polarized XUV light at an incidence angle of 60.4° (Brewster angle for 800 nm radiation).

determination of the optical frequencies. However, applicability of our XUV frequency comb for high resolution laser spectroscopy relies on the coherence of the generation process. So far there was only indirect evidence that this is indeed the case. For example, it was observed that two independent HHG sources pumped by the same fundamental pulse produce stable interference fringes[22] and that the generated XUV bursts are compressible[23], which both indicate that the phase link between fundamental and XUV is tight. Direct evidence can only be provided by a beat measurement between two independent XUV sources or a spectroscopy measurement. Upconversion of phase noise in the fundamental pulse train that might bury the comb is reduced in our approach, as the enhancement resonator acts as a flywheel for the incoming pulse train.

When the buildup resonator (shown in Fig. 1 and explained in the Methods section) is put into lock and the CE frequency of the laser is adjusted to maximize the power inside the resonator, an optical spectrum as shown in Fig. 2 is observed. The circulating (average) power has been determined to be 38 W. The discrepancy between the calculated ($P = 100$) and observed enhancement ($P = 54$) can mostly be attributed to spectral filtering due to residual dispersion inside the resonator. The autocorrelation of the stored pulse inside the resonator is measured using the residual reflection of the fundamental laser radiation from the first Brewster window (see Fig. 1). It indicates an approximately chirp-free pulse of about 28 fs duration. With these figures, we estimate a peak power of about 12 MW and intensities in the focus of around 5×10^{13} W cm^{-2}. Turning on the xenon jet has no effect on the cavity lock, which shows that plasma induced phase noise above feedback bandwidth (10 kHz) is negligible.

Given these conditions, an XUV spectrum as shown in Fig. 3 can be observed after the XUV output coupler, which is described in the Methods section. High harmonics up to fifteenth order or 23 eV photon energy (as expected for these intensities) are observed, with an exponential roll-off starting around the ninth harmonic, presumably due to increasing phase mismatch. The cut-off wavelength of our XUV spectrometer around 120 nm prevented us from observing the fifth harmonic. The third harmonic could be observed with the naked eye, even though the outcoupling efficiency was very low for this wavelength. Additionally, we observe a line slightly below the ionization potential of xenon at 103 nm, which to our knowledge has not been reported previously. To test the comb coherence, we performed a beat experiment between the third harmonic from the

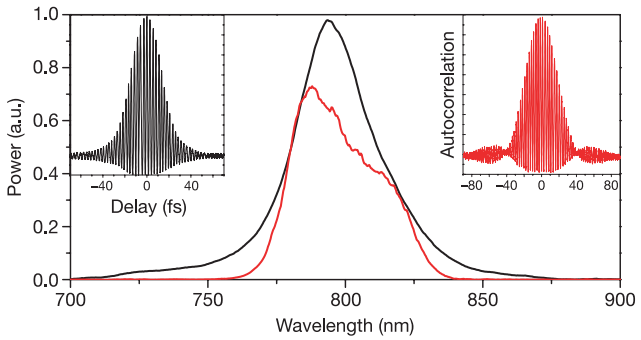

Figure 2 | Normalized spectrum of the pump laser (black) and the circulating pulse in the enhancement resonator (red) when locked. Inset, respective measured autocorrelations.

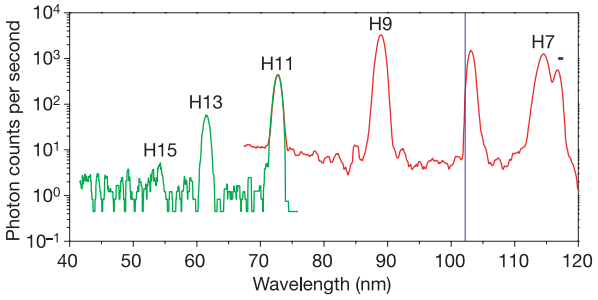

Figure 3 | Harmonic spectrum obtained with the resonator locked and the xenon jet on. The short-wavelength end of the spectrum (green) is taken with a 0.1 μm aluminium filter in the beam path to reduce stray light from the stronger lower harmonics, and is rescaled to match the peak height at the eleventh harmonic (H11) of the measurement without filter (red). Blue dots indicate the 5P–7S resonance in xenon that modifies the shape of the seventh harmonic (H7), and the vertical line indicates the ionization potential. The spectral feature just below the ionization limit presumably originates from fluorescence of coherently excited Rydberg states.

enhancement cavity and the fourth harmonic of a mode-locked Nd:YVO_4 laser. The results are shown in Fig. 4. A similar result[24] is obtained in a beat measurement between third harmonics produced in a nonlinear crystal and a gas jet, which proves equation (2) for this special case.

In order to test the spatial coherence of the harmonic radiation and investigate the possible origin of the feature at 103 nm, we have recorded transverse beam profiles for each feature of the spectrum from the seventh through to the eleventh harmonic by translating the monochromator in the horizontal direction and recording the transmitted intensity for each feature. A gaussian fit to these profiles yields divergence angles of 14, 11 and 10 mrad for the seventh, ninth and eleventh harmonic, respectively. This corresponds approximately to the diffraction limit, which would allow tight focusing. The divergence of the feature at 103 nm could not be determined, as it exceeds the limited viewing angle of the set-up.

We also investigated the generated power of the different spectral features as a function of the fundamental power. The results are shown in Fig. 5. As expected[25], for low intensities before the individual harmonic reaches the plateau, it follows a power law with an exponent close to the harmonic order. As the harmonic reaches the plateau, the exponent decreases to a value that is approximately the same for all harmonic orders. The line at 103 nm exhibits a very high slope for low intensities while it quickly saturates and even decreases at higher powers, which, in addition to the divergence and the frequency not being close to an odd harmonic, suggests that a different process than the usual HHG is responsible for that feature. A possible explanation for this feature would be that during the pulse the Rydberg levels of the atom are Stark-shifted into eight- and even nine-photon resonance with the fundamental laser light. Population can accumulate there, as high-lying Rydberg states are robust against field ionization for such short laser pulses. This long-lived excited dipole can now oscillate for a long time in phase even after the pulse has passed, so that most of the emitted power is directed and has a frequency of the unperturbed Rydberg states just below the ionization limit.

The total power of the spectral range from 120 nm down to 60 nm was determined to be more than 1 nW after the sapphire window. If the calculated coupling efficiency of that window is taken into account, more than 10^{-8} of the power from the laser is converted into photons in the 60–120 nm range. Optimized results with chirped pulse amplifier (CPA) systems reached more than 10^{-5} single pass efficiency in this wavelength range[26]. With the advent of precision dispersion characterization[27], dispersion-compensated resonators with enhancement factors of 1,000 are possible, so that with high energy oscillators[28], intra-cavity pulse energies approaching 100 μJ seem realistic with current technologies. Obviously, at such high pulse energies, special care has to be taken to avoid nonlinear responses of such a resonator, such as self phase modulation in windows, two-photon absorption in the mirror coatings, and the like. In this case optimized single pass conversion efficiencies would allow a total power conversion in the per cent range and XUV output powers in the mW range.

In conclusion, we have shown that efficient high-order harmonic generation directly from a Ti:sapphire oscillator is possible by use of an enhancement resonator of high finesse specifically designed to support ultrashort femtosecond pulses. This not only reduces the complexity of the set-up for the generation of high harmonics compared to a typical CPA system but simultaneously increases the repetition rate of this conversion by several orders of magnitude. At such a high repetition rate, the frequency comb from the fundamental laser will also be usable in the XUV, so that high resolution spectroscopy in the XUV comes into reach. This will enable new high precision tests for fundamental physical theories. For example, the 1S–2S transition of singly charged helium can be probed with the thirteenth harmonic of a Ti:sapphire laser. This would provide an even more sensitive test of quantum electrodynamics than the hydrogen 1S–2S experiment[29]. If these measurements are combined, a new precise value for the proton charge radius and the Rydberg constant may be obtained. It can be expected that the presented method is capable of producing orders of magnitude more intense XUV output than conventional HHG schemes and with excellent spatial coherence, so that other applications like XUV interferometry, holography and lithography come into the realm of reality.

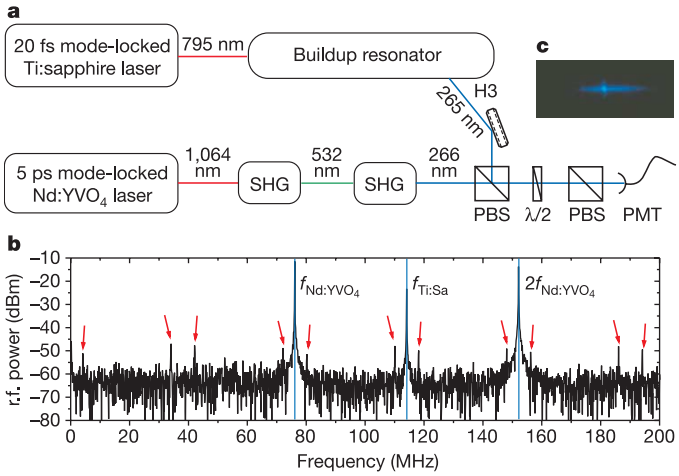

Figure 4 | Frequency comb coherence. **a**, Set-up for testing comb coherence at the third harmonic (H3). SHG, second harmonic generation; PBS, polarizing beam splitter; PMT, photomultiplier. To synchronize the two lasers, the third harmonic of the Nd:YVO_4 laser repetition rate (76 MHz) was phase-locked to the second harmonic of the Ti:sapphire laser repetition rate (changed to 114 MHz). The repetition rates from the two lasers are marked with blue lines in the r.f. spectrum (**b**). The red arrows mark the position of the beat signals observed when the delay between the pulses is adjusted appropriately using an r.f. delay line. **c**, Grating image of the overlapped beams with the narrow bandwidth picosecond laser (bright spot) confined to the centre of the femtosecond spectrum.

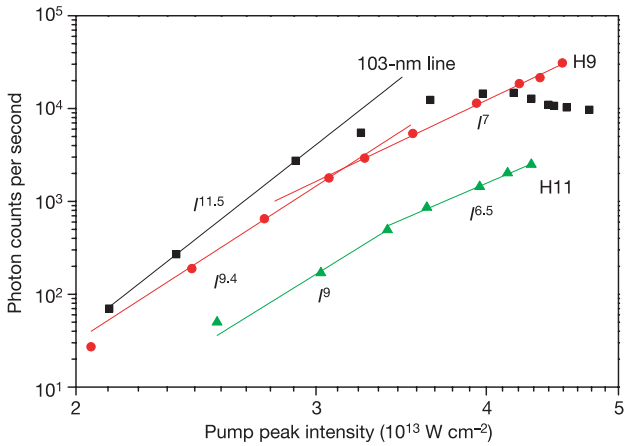

Figure 5 | Generated power versus the fundamental intensity *I* for three spectral features. Data are shown for the feature at 103 nm (squares), the ninth harmonic (H9; circles) and the eleventh harmonic (H11; triangles). Solid lines represent fits to the data with a power law with exponents as indicated. The ninth harmonic follows a power law with an exponent of 9.4 for low intensities, as expected from lowest order perturbation theory, whereas for higher powers it decreases to 7. The eleventh harmonic shows a similar behaviour, with the change in exponent occurring at a higher intensity. The line at 103 nm shows a high exponent of 11.5 for low intensities and then quickly saturates (and even decreases).

METHODS

Apparatus. The complete set-up is sketched in Fig. 1, and consists of a Ti:sapphire femtosecond oscillator (Femtolasers Femtosource 20) that delivers 20 fs pulses with 850 mW average power at 800 nm and a repetition rate of 112 MHz, which results in a pulse energy of 7.7 nJ and a peak power around 400 kW. These pulses are sent to the enhancement resonator, which is a bowtie-type ring cavity. It consists of eight mirrors: a 1% transmission coupling mirror; a 1/4-inch mirror mounted on a piezoelectric transducer for electronic control of the cavity length using the polarization lock technique[30]; four plane chirped mirrors for compensation of the dispersion of air; and the two sapphire Brewster windows inside the resonator. Two spherical mirrors with 50 mm focal length produce a tight focus with a diameter of about 5.3 μm inside the harmonic generation chamber. On the way to the resonator, the beam passes through a prism compressor that compensates the dispersion of the coupling mirror substrates and a telescope that matches the beam diameter and focus position to the resonator mode. In this way, nearly transform limited pulses are obtained inside the resonator. For optimal coupling the enhancement resonator input mirror has 1% transmission, so that an enhancement factor of $P = 100$ is expected. The laser resonator includes a pair of thin wedged fused silica plates for manual control of the carrier envelope frequency. No electronic feedback was necessary to control the CE frequency of the laser, because the system was stable enough to operate for hours by feeding back on the resonator length only. The power circulating in the resonator while put into lock was determined by measuring the power leaking through one of the highly reflecting cavity mirrors with accurately known spectral transmission. The intra-cavity spectrum was measured the same way. Amplitude stability was better than 10% r.m.s. with no frequencies higher than 1 MHz limited by photon lifetime.

Procedure. The enhancement resonator contains a small vacuum chamber with Brewster-angled sapphire windows, housing the rare-gas jet. The peak intensity in these windows is smaller than 10 GW cm^{-2}, so that their nonlinear response is negligible. Xenon gas is injected into the focus of the resonator mode in the HHG chamber, using a glass capillary placed right above the focus with approximately 50 μm inner diameter and 1 bar backing pressure. This diameter is approximately matched to the Rayleigh range of the focus of about 110 μm. With this focus geometry and repetition rate, the atoms see about five pulses before leaving the focus. As the coherently generated XUV radiation is emitted collinearly with the fundamental in a well-collimated beam, a crucial component in the scheme is some sort of beam splitter that separates the two. In order not to compromise the resonator finesse, this beam splitter has to have a very low loss for the fundamental laser radiation. The vacuum windows fulfill this requirement through Brewster orientation with losses smaller than 10^{-3} per window, and accomplish the separation by providing total external reflection for the XUV. High Fresnel reflectivity (inset in Fig. 1) is achieved in this range, as the refractive index of sapphire is lower than one for the relevant wavelengths. The generated XUV beam extracted this way was analysed with a grazing incidence XUV monochromator (McPherson model 248/310G) placed at the HHG chamber exit port. A channeltron photodetector (BURLE CEM4751G), sensitive to wavelengths below 150 nm, was installed at the exit slit of the monochromator, and its signal was analysed with (1) a photon counter (Stanford Research SR400) for high sensitivity measurements, and (2) a voltmeter across a 1 MΩ load resistance for XUV photon flux measurements. To determine the total power in the observed XUV spectrum, the channeltron was placed directly in the beam at the XUV port. A photocurrent of 1 μA was detected at 1.36 kV bias, which corresponds to a photon flux of about 0.85×10^9 photons per second, according to the manufacturer's specifications. From the spectrum we know that the major contributions to that flux come from the spectral range between 85 and 115 nm, so that we can assume an average photon energy of about 12 eV, from which the total power can be calculated.

To synchronise the two lasers in the beat experiment, the third harmonic of the Nd:YVO_4 laser repetition rate (76 MHz) was phase-locked to the second harmonic of the Ti:sapphire laser repetition rate (changed to 114 MHz). The delay between the pulses from the two lasers was adjusted using an r.f. phase shifter. The beat signal was recorded using a photomultiplier tube.

Received 15 March; accepted 23 May 2005.

1. Udem, T., Holzwarth, R. & Hänsch, T. W. Optical frequency metrology. *Nature* **416,** 233–237 (2002).
2. Cundiff, S. T. & Ye, J. Femtosecond optical frequency combs. *Rev. Mod. Phys.* **75,** 325–342 (2003).
3. Diddams, S. A. *et al.* An optical clock based on a single trapped $^{199}Hg^+$ ion. *Science* **293,** 825–828 (2001).
4. Baltuška, A. *et al.* Attosecond control of electronic processes by intense light fields. *Nature* **421,** 611–615 (2003).
5. Goulielmakis, E. *et al.* Direct measurement of light waves. *Science* **305,** 1267–1269 (2004).
6. Lindner, F. *et al.* High-order harmonic generation at a repetition rate of 100 kHz. *Phys. Rev. A* **68,** 013814 (2003).
7. Rafac, R. J. *et al.* Sub-dekahertz ultraviolet spectroscopy of $^{199}Hg^+$. *Phys. Rev. Lett.* **85,** 2462–2465 (2000).
8. Strickland, D. & Mourou, G. Compression of amplified chirped optical pulses. *Opt. Commun.* **56,** 219–221 (1985).
9. Seres, J. *et al.* Laser technology: Source of coherent kiloelectronvolt X-rays. *Nature* **433,** 596 (2005).
10. Schoof, A., Grünert, J., Ritter, S. & Hemmerich, A. Reducing the linewidth of a diode laser below 30 Hz by stabilization to a reference cavity with a finesse above 10^5. *Opt. Lett.* **26,** 1562–1564 (2001).
11. Polzik, E. S. & Kimble, H. J. Frequency doubling with $KNbO_3$ in an external cavity. *Opt. Lett.* **16,** 1400–1402 (1991).
12. Reichert, J., Holzwarth, R., Udem, T. & Hänsch, T. W. Measuring the frequency of light with mode-locked lasers. *Opt. Commun.* **172,** 59–68 (1999).
13. Jones, R. J. & Ye, J. Femtosecond pulse amplification by coherent addition in a passive optical cavity. *Opt. Lett.* **27,** 1848–1850 (2002).
14. Petersen, J. C. & Luiten, A. N. Short pulses in optical resonators. *Opt. Express* **11,** 2975–2981 (2003).
15. Yanovsky, V. P. & Wise, F. W. Frequency doubling of 100-fs pulses with 50% efficiency by use of a resonant enhancement cavity. *Opt. Lett.* **19,** 1952–1954 (1994).
16. Jones, R. J. & Ye, J. High-repetition-rate coherent femtosecond pulse amplification with an external passive optical cavity. *Opt. Lett.* **29,** 2812–2814 (2004).
17. Baklanov, Y. V. & Chebotayev, V. P. Narrow resonances of 2-photon absorption of super-narrow pulses in a gas. *Appl. Phys.* **12,** 97–99 (1977).
18. Snadden, M. J., Bell, A. S., Riis, E. & Ferguson, A. I. Two-photon spectroscopy of laser-cooled Rb using a mode-locked laser. *Opt. Commun.* **125,** 70–76 (1996).
19. Eckstein, J. N., Ferguson, A. I. & Hänsch, T. W. High-resolution spectroscopy with ultrashort light-pulses. *J. Opt. Soc. Am.* **68,** 646 (1978).
20. Marian, A., Stowe, M. C., Lawall, J. R., Felinto, D. & Ye, J. United time-frequency spectroscopy for dynamics and global structure. *Science* **306,** 2063–2068 (2004).
21. Witte, S., Zinkstok, R. T., Ubachs, W., Hogervorst, W. & Eikema, K. S. E. Deep-ultraviolet quantum interference metrology with ultrashort laser pulses. *Science* **307,** 400–403 (2005).
22. Bellini, M. *et al.* Temporal coherence of ultrashort high-order harmonic pulses. *Phys. Rev. Lett.* **81,** 297–300 (1998).
23. López-Martens, R. *et al.* Amplitude and phase control of attosecond light pulses. *Phys. Rev. Lett.* **94,** 033001 (2005).
24. Jones, R. J., Moll, K., Thorpe, M., Ye, J. Phase-coherent frequency combs in the vacuum ultraviolet via high-harmonic generation inside a femtosecond enhancement cavity. *Phys. Rev. Lett.* **94,** 193201 (2005).
25. Wahlström, C. G. *et al.* High-order harmonic-generation in rare-gases with an intense short-pulse laser. *Phys. Rev. A* **48,** 4709–4720 (1993).
26. Constant, E. *et al.* Optimizing high harmonic generation in absorbing gases: Model and experiment. *Phys. Rev. Lett.* **82,** 1668–1671 (1999).
27. Thorpe, M. J., Jason, J. R., Moll, K., Ye, J. & Lalezari, R. Precise measurements of optical cavity dispersion and mirror coating properties via femtosecond combs. *Opt. Expr.* **13,** 882–888 (2005).
28. Fernandez, A. *et al.* Chirped-pulse oscillators: a route to high-power femtosecond pulses without external amplification. *Opt. Lett.* **29,** 1366–1368 (2004).
29. Fischer, M. *et al.* New limits on the drift of fundamental constants from laboratory measurements. *Phys. Rev. Lett.* **92,** 230802 (2004).
30. Hänsch, T. W. & Couillaud, B. Laser frequency stabilization by polarization spectroscopy of a reflecting reference cavity. *Opt. Commun.* **35,** 441–444 (1980).

Acknowledgements We thank A. Apolonski and M. Yu. Ivanov for discussions, and E. Seres and J. Seres for lending us the XUV monochromator.

Author Information Reprints and permissions information is available at npg.nature.com/reprintsandpermissions. The authors declare no competing financial interests. Correspondence and requests for materials should be addressed to C.G. (ctg@mpq.mpg.de).